Metal Requirements of a Diadenosine Pyrophosphatase from *Bartonella bacilliformis*: Magnetic Resonance and Kinetic Studies of the Role of Mn^{2+} †

G. Bernard Conyers,‡ Gong Wu,§ Maurice J. Bessman,|| and Albert S. Mildvan*,§

Departments of Biology and Biophysics and the McCollum−Pratt Institute, The Johns Hopkins University, 3400 North Charles Street, Baltimore, Maryland 21218, and Department of Biological Chemistry, The Johns Hopkins School of Medicine, 725 North Wolfe Street, Baltimore, Maryland 21205-2185

Received October 22, 1999; Revised Manuscript Received December 16, 1999

ABSTRACT: Recombinant IalA protein from *Bartonella bacilliformis* is a monomeric adenosine 5′-tetraphospho-5′-adenosine (Ap_4A) pyrophosphatase of 170 amino acids that catalyzes the hydrolysis of Ap_4A, Ap_5A, and Ap_6A by attack at the δ-phosphorus, with the departure of ATP as the leaving group [Cartwright et al. (1999) *Biochem. Biophys. Res. Commun. 256*, 474−479]. When various divalent cations were tested over a 300-fold concentration range, Mg^{2+}, Mn^{2+}, and Zn^{2+} ions were found to activate the enzyme, while Ca^{2+} did not. Sigmoidal activation curves were observed with Mn^{2+} and Mg^{2+} with Hill coefficients of 3.0 and 1.6 and $K_{0.5}$ values of 0.9 and 5.3 mM, respectively. The substrate $M^{2+}\cdot Ap_4A$ showed hyperbolic kinetics with K_m values of 0.34 mM for both $Mn^{2+}\cdot Ap_4A$ and $Mg^{2+}\cdot Ap_4A$. Direct Mn^{2+} binding studies by electron paramagnetic resonance (EPR) and by the enhancement of the longitudinal relaxation rate of water protons revealed two Mn^{2+} binding sites per molecule of Ap_4A pyrophosphatase with dissociation constants of 1.1 mM, comparable to the kinetically determined $K_{0.5}$ value of Mn^{2+}. The enhancement factor of the longitudinal relaxation rate of water protons due to bound Mn^{2+} (ϵ_b) decreased with increasing site occupancy from a value of 12.9 with one site occupied to 3.3 when both are occupied, indicating site−site interaction between the two enzyme-bound Mn^{2+} ions. Assuming the decrease in ϵ_b to result from cross-relaxation between the two bound Mn^{2+} ions yields an estimated distance of 5.9 ± 0.4 Å between them. The substrate Ap_4A binds one Mn^{2+} (K_d = 0.43 mM) with an ϵ_b value of 2.6, consistent with the molecular weight of the $Mn^{2+}\cdot Ap_4A$ complex. Mg^{2+} binding studies, in competition with Mn^{2+}, reveal two Mg^{2+} binding sites on the enzyme with K_d values of 8.6 mM and one Mg^{2+} binding site on Ap_4A with a K_d of 3.9 mM, values that are comparable to the $K_{0.5}$ for Mg^{2+}. Hence, with both Mn^{2+} and Mg^{2+}, a total of three metal binding sites were found—two on the enzyme and one on the substrate—with dissociation constants comparable to the kinetically determined $K_{0.5}$ values, suggesting a role in catalysis for three bound divalent cations. Ca^{2+} does not activate Ap_4A pyrophosphatase but inhibits the Mn^{2+}-activated enzyme competitively with a $K_i = 1.9 \pm 1.3$ mM. Ca^{2+} binding studies, in competition with Mn^{2+}, revealed two sites on the enzyme with dissociation constants (4.3 ± 1.3 mM) and one on Ap_4A with a dissociation constant of 2.1 mM. These values are similar to its K_i suggesting that inhibition by Ca^{2+} results from the complete displacement of Mn^{2+} from the active site. Unlike the homologous MutT pyrophosphohydrolase, which requires only *one* enzyme-bound divalent cation in an $E\cdot M^{2+}\cdot NTP\cdot M^{2+}$ complex for catalytic activity, Ap_4A pyrophosphatase requires *two* enzyme-bound divalent cations that function in an active $E\cdot(M^{2+})_2\cdot Ap_4A\cdot M^{2+}$ complex.

Nudix hydrolases are metal-requiring enzymes that hydrolyze a wide variety of nucleoside diphosphate derivatives and possess a highly conserved signature sequence called the Nudix box: $GX_5EX_7REUXEEXGU$, where U is a hydrophobic residue (*1*). The solution structure of the MutT enzyme, the only known structure of a member of this family, showed the Nudix box to form a loop I−helix I−loop II motif that contributes liganding residues for the essential enzyme-bound divalent cation, as well as catalytic residues (*2*, *3*). Searches for the Nudix box in protein sequence databases show that over 300 putative Nudix hydrolases are widely distributed in all kingdoms.

This paper examines a Nudix hydrolase from *Bartonella bacilliformis*, which is the only known bacterium that invades erythrocytes and is the causative agent of several serious blood and skin diseases in man (*4*). Using a genetic approach, Mitchell and Minnick have associated the hemolytic invasive abilities of this organism with a two-gene invasion-associated locus *ialAB* (*5*), which contains an open reading frame (*ialA*) that codes for a Nudix hydrolase (*6*). The IalA protein from *B. bacilliformis*, which is essential for the invasion of

† This research was supported by the National Institutes of Health Grant DK 28616 to A.S.M., by the National Institutes of Health Grant GM 18649 to M.J.B., and by the National Institutes of Health Fellowship GM-17178 to G.B.C.

* Address correspondence to this author: Tel 410-955-2038; Fax 410-955-5759; e-mail mildvan@welchlink.welch.jhu.edu.

‡ Biophysics Department, The Johns Hopkins University.

§ The Johns Hopkins School of Medicine.

|| Biology Department and The McCollum−Pratt Institute, The Johns Hopkins University.

10.1021/bi992458n CCC: $19.00
Published on Web 02/12/2000

erythrocytes by the bacterium (*5*), is a monomeric Ap_4A[1] pyrophosphatase of molecular weight 20 100 that catalyzes the reaction (*7, 8*)

$$Ap_nA^{-n} + H_2O \rightarrow ATP^{-4} + AP_{(n-3)}^{-(n-2)} + 2H^+ \quad (1)$$

where $6 \geq n \geq 4$. While several Ap_4A-degrading enzymes from eukaryotic organisms exist that cleave Ap_4A asymmetrically, the Ap_4A pyrophosphatase from *B. bacilliformis* is the only known enzyme from a prokaryotic organism that cleaves Ap_4A asymmetrically (*9*−*14*). The Nudix box may account for this asymmetrical cleavage.

Using ^{18}O NMR labeling experiments, Cartwright et al. (*8*) have shown that the Ap_4A pyrophosphatase reaction occurs by nucleophilic substitution at the δ-phosphorus atom of Ap_4A. By the same method, a similar observation was made with an asymmetrical Ap_4A-degrading enzyme from yellow-lupin seeds, which also possesses a Nudix box (*9*). Symmetrical Ap_4A-degrading enzymes from bacterial sources characterized so far do not possess a Nudix box and may use a different mechanism. For example, Ap_4A pyrophosphatase from *Escherichia coli* produces two molecules of ADP and is incapable of cleaving an Ap_4A analogue where the central oxygen atom was replaced by a carbon atom (*15*). The nucleotide Ap_4A has been implicated in signal transduction and in metabolic regulation (*16*), providing a tool for understanding the regulation of pathways involved in the invasion process by hemolytic bacteria. The asymmetrically cleaving Ap_4A pyrophosphatase from *B. bacilliformis* provides the first evidence that an alternate pathway for Ap_4A degradation and ATP production exists in some bacteria (*7, 8*).

Nudix hydrolases have an absolute requirement for divalent metal ion cofactors such as Mg^{2+} or Mn^{2+}. The precise roles of the divalent cations have been clarified for only one Nudix enzyme (*2, 17*), the MutT pyrophosphohydrolase from *E. coli*, which hydrolyzes nucleoside triphosphates (NTPs) to NMP and pyrophosphate (*18*). A total of two divalent cations are required for activity of the MutT enzyme, one coordinated by the β- and γ-phosphoryl groups of the NTP substrate and the other coordinated by Gly-38, and Glu-56, -57, and -98 of the enzyme (*2, 17*). The metal−nucleotide substrate binds in the second coordination sphere of the enzyme-bound metal to form a quaternary $E{\cdot}M^{2+}{\cdot}(H_2O){\cdot}NTP{\cdot}M^{2+}$ complex (*2*). By mutagenesis of the metal ligands, the enzyme-bound divalent cation has been found to contribute a factor of $\geq 10^5$ to catalysis (*3, 19*). While the products of most Nudix enzymes are NMP and another phosphorylated moiety, *B. bacilliformis* Ap_4A pyrophosphatase differs in that it asymmetrically hydrolyzes Ap_4A and Ap_5A to produce one molecule of ATP and symmetrically hydrolyzes Ap_6A to produce two molecules of ATP. Studies of prokaryotic and eukaryotic Ap_4A pyrophosphatases show that nearly all require divalent cations for activity. An exception is the enzyme from *Physarum polycephalum*, although tightly bound metal ions have not been excluded (*13*).

In no case of an Ap_4A pyrophosphatase has the precise role of the essential metal ion(s) been determined. For these reasons, the role of divalent cations in the Ap_4A pyrophosphatase from *B. bacilliformis* was investigated by kinetic and metal binding studies using EPR and water relaxation methods (*20, 21*) with Mn^{2+} and Mg^{2+} as the metal activators. The results indicate that, unlike the MutT enzyme, Ap_4A pyrophosphatase uses a total of three divalent cations for catalysis, two coordinated by the enzyme and one by the substrate.

EXPERIMENTAL PROCEDURES

Materials. Recombinant Ap_4A pyrophosphatase from *B. bacilliformis* was prepared as previously described (*7*). SDS−PAGE showed the final fraction IV obtained by this procedure to be at least 95% homogeneous. For use in the magnetic resonance experiments, fraction IV was concentrated into 50 mM Tris-HCl, pH 7.5, that had been treated with Chelex-100 (Bio-Rad) to remove trace metal contaminants. Ap_4A was purchased from Sigma and solutions were treated with Chelex-100. All compounds were the purest commercially available.

General Methods. Unless otherwise stated, all kinetic and thermodynamic experiments were done at 23 °C. Protein was analyzed by SDS−PAGE on a 15% resolving gel with a 5% stacking layer on a vertical electrophoresis apparatus obtained from Gibco. The concentration of protein was determined by a Bradford assay (Bio-Rad Laboratories, Richmond, CA) using bovine serum albumin as a standard. Kinetic data were obtained on a Hitachi U-200 spectrophotometer thermostated at 23 °C. The kinetic data were fit by nonlinear least-squares regression analysis to the Michaelis−Menten equation by use of Enzyme Kinetics V1.5 (Trinity Software). Binding data were fitted by nonlinear regression analysis by use of the Grafit program (Erithacus Software Ltd., Staines, U.K.).

Kinetic Studies. The enzyme assay measures the conversion of a phosphatase-insensitive substrate (Ap_4A) to a phosphatase-sensitive substrate (AMP or ATP) in 50 μL containing 50 mM Tris-HCl, pH 7.5, 9 units of calf intestinal alkaline phosphatase, and 0.1−1.5 milliunit of Ap_4A pyrophosphatase (*7*). For studies of enzyme activation by Mn^{2+}, the reaction mixtures contained Ap_4A concentrations of 0.75 and 1.0 mM and variable $MnCl_2$ concentrations ranging from 0.012 to 3.5 mM. For studies of activation by Mg^{2+}, Ap_4A concentrations of 1.0, 2.0, 5.0, and 7.0 mM were used with $MgCl_2$ concentrations ranging from 0.25 to 20.0 mM. For measurements of the K_m of Ap_4A with Mn^{2+}, the concentration of $MnCl_2$ was 3.0 mM and that of Ap_4A was varied from 0.06 to 1.0 mM. With Mg^{2+} as the activator, the $MgCl_2$ concentration was 20.0 mM and the Ap_4A concentration was varied from 0.04 to 1.0 mM. The reactions were initiated by the addition of Ap_4A pyrophosphatase and terminated after 15−60 min by the addition of 250 μL of 12 mM EDTA. The solutions were analyzed for the presence of inorganic orthophosphate from the hydrolysis of the products AMP and ATP by alkaline phosphatase, using the method of Ames and Dubin (*22*). A unit of activity is defined as 1 μmol of substrate hydrolyzed/min. Under these conditions, the velocity of the reaction was linear with time and with enzyme concentration. Hyperbolic activation curves by the substrate, Ap_4A, were fit by nonlinear least-squares regression analysis to the Michaelis−Menten equation to yield K_m and V_{max} values. Sigmoidal activation curves, found with $MnCl_2$ and

[1] Abbreviations: Ap_4A, adenosine 5′-tetraphospho-5′-adenosine (other members of this class are abbreviated in an analogous fashion); EPR, electron paramagnetic resonance; PRR, water proton relaxation rate.

$MgCl_2$, were fit to the Hill equation to yield the Hill coefficient (n_H), $K_{0.5}$, and V_{max}:

$$v = \frac{V_{max}[M]^{n_H}}{[K_{0.5}]^{n_H} + [M]^{n_H}} \quad (2)$$

Binding Studies. The binding of the paramagnetic ion Mn^{2+} to the substrate Ap_4A and to the enzyme was studied by EPR spectroscopy, which measures the concentration of free Mn^{2+} (*23*), and independently by the enhancement of the longitudinal proton relaxation rate (PRR) of water, which measures a property of bound Mn^{2+} (*21*). To determine the K_d of $Mn^{2+}\cdot Ap_4A$, $MnCl_2$ (60 μM) was titrated with Ap_4A (30−700 μM). To study Mn^{2+} binding to the enzyme, 400 μM Ap_4A pyrophosphatase was titrated with $MnCl_2$ (500−3500 μM). Titrations were carried out in 40 μL volumes containing 50 mM Tris-HCl, pH 7.5. Both EPR and PRR measurements were made on the same samples at 23 °C. The EPR measurements were made with a Varian E-4 EPR spectrometer at 9.1 GHz and analyzed by Scatchard plots to yield the stoichiometry and dissociation constants of the Mn^{2+}−ligand complexes. The longitudinal proton relaxation rate of water was measured at 24.3 MHz with a Seimco pulsed NMR spectrometer using a 180°−τ−90° pulse sequence as described previously (*21, 24*). The observed enhancement (ϵ*) of the longitudinal proton relaxation rate by enzyme-bound Mn^{2+} is defined as

$$\epsilon^* = \frac{1/T_1^* - 1/T_{1,0}^*}{1/T_1 - 1/T_{1,0}} \quad (3)$$

where $1/T_1$ and $1/T_{1,0}$ are the longitudinal relaxation rates of water protons in the presence and absence of Mn^{2+} and $1/T_1$* and $1/T_{1,0}$* represent the same parameters in the presence of enzyme. From the observed enhancement factor (ϵ*) and the concentration of free Mn^{2+} measured by EPR ($[Mn^{2+}]_f$), the enhancement of the bound Mn^{2+} (ϵ_b) was calculated:

$$\epsilon^* = \frac{[Mn^{2+}]_f}{[Mn^{2+}]_t}\epsilon_f + \frac{[Mn^{2+}]_b}{[Mn^{2+}]_t}\epsilon_b \quad (4)$$

where the subscripts t, f, and b refer to the total, free, and bound concentration of Mn^{2+} and $[Mn^{2+}]_t = [Mn^{2+}]_f + [Mn^{2+}]_b$. The enhancement of free Mn^{2+} (ϵ_f) is defined as unity (*20, 21*).

Mg^{2+} and Ca^{2+} Binding Studies. Displacement of Mn^{2+} from $Mn^{2+}\cdot$enzyme or $Mn^{2+}\cdot$nucleotide complexes by another metal ion decreases the observed enhancement factor ϵ* and increases the concentration of free Mn^{2+}. If the competing ion is diamagnetic (e.g., Mg^{2+} or Ca^{2+}), titrations of a solution of Mn^{2+} and ligand with a second metal ion can be used to obtain the dissociation constant of the second metal ion. Both PRR and EPR were used to study the competitive binding of Mg^{2+} and Ca^{2+} to both Ap_4A and to Ap_4A pyrophosphatase. The concentration of free Mg^{2+} that caused half-maximal displacement of Mn^{2+} from the enzyme

$$[Mg^{2+}]_f^{50\%} = [Mg^{2+}]_f - \frac{[\text{enzyme sites}]}{2} \quad (5)$$

was used to determine the dissociation constant of Mg^{2+} ($K_d^{Mg^{2+}}$) from the enzyme:

$$K_d^{Mg^{2+}} = \frac{[Mg^{2+}]_f^{50\%}}{1 + \dfrac{[Mn^{2+}]_f^{50\%}}{K_d^{Mn^{2+}}}} \quad (6)$$

In eq 6, $[Mn^{2+}]_f^{50\%}$ is the concentration of free Mn^{2+} at half-maximal displacement and $K_d^{Mn^{2+}}$ is the dissociation constant of Mn^{2+} that was determined independently as described above. Equations analogous to eqs 5 and 6 were used to determine the dissociation constants of the $Mg^{2+}\cdot Ap_4A$ complex, the $Ca^{2+}\cdot Ap_4A$ complex, and the $Ca^{2+}\cdot$enzyme complex.

Table 1: Effects of Various Metal Ions on Ap_4A Pyrophosphatase Activity[a]

metal salt	relative activity[b]					
	0.1 mM	0.3 mM	1 mM	3 mM	10 mM	30 mM
$MgCl_2$	< 1	< 1	< 1	18	58	100
$MnCl_2$	< 1	< 1	22	93	68	37
$ZnCl_2$	< 1	23	117	94	51	58
$CaCl_2$	< 1	< 1	< 1	< 1	< 1	< 1

[a] Conditions: 50 mM Tris-HCl, pH 7.5, 1.0 mM Ap_4A, 9.0 units of calf intestinal alkaline phosphatase, and 0.35 milliunit of Ap_4A pyrophosphatase in a total volume of 50 μL at 37 °C. [b] Activity is relative to the maximal activity with Mg^{2+}.

RESULTS

Effects of Divalent Cations on the Activity of Ap_4A Pyrophosphatase. Table 1 lists four divalent cations that were tested over a 300-fold range (0.10−30.0 mM) as activators of Ap_4A pyrophosphatase. The data indicated that while Mg^{2+}, Mn^{2+}, and Zn^{2+} activated Ap_4A hydrolysis, Ca^{2+} did not. Inhibition by Mn^{2+} and Zn^{2+} was found when the concentrations of these metals exceeded 3 mM, possibly due to binding at additional sites on the enzyme or substrate. No such inhibition was seen at high Mg^{2+} concentrations. While Ca^{2+} did not activate the enzyme, it was found to be a competitive inhibitor with respect to activating divalent cations (see below). While the total Zn^{2+} content of mammalian cells is 196−260 μM, almost all of the Zn^{2+} is tightly bound to metalloproteins (*25*−*27*). Similarly, the total Mn^{2+} content of hepatocytes is 34 μM, of which only 0.7 μM is free (*28*). The total cell Mg^{2+} levels range from 3.5 to 8.5 mM, of which 0.5−1.0 mM is free (*29*). Since Mg^{2+} is less tightly bound to proteins and other ligands than Zn^{2+} or Mn^{2+}, Mg^{2+} is the likely in vivo metal activator of Ap_4A pyrophosphatase. Hence Zn^{2+} was not studied further. Because of its value as a paramagnetic probe and an activator, Mn^{2+} was used for kinetic and metal binding studies.

Binding of Mn^{2+}, Mg^{2+}, and Ca^{2+} to Ap_4A. It was first necessary to determine the dissociation constant of the binary $Mn^{2+}\cdot Ap_4A$ complex under the conditions of the kinetic experiments. The determination was done by two independent methods, EPR, which measures the concentration of free Mn^{2+} ions, and the enhancement (ϵ*) of the longitudinal proton relaxation rate (PRR) of water, which measures a property of bound Mn^{2+}. The EPR data (not shown) yielded a K_d of 497 ± 88 μM for the binary $Mn^{2+}\cdot Ap_4A$ complex, and the PRR data yielded a similar K_d of 363 ± 206 μM

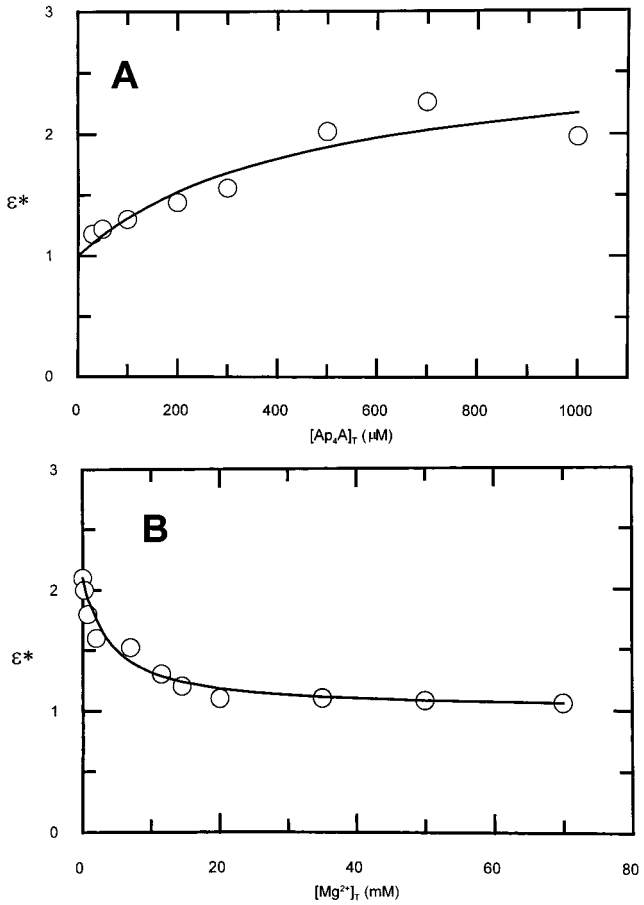

FIGURE 1: Divalent cation binding to Ap_4A. (A) Mn^{2+} binding. Titration of 60 μM $MnCl_2$ with Ap_4A showing the enhancement (ϵ*) of the PRR of water. (B) Mg^{2+} binding in competition with Mn^{2+}. Titration of 0.40 mM $MnCl_2$ and 0.70 mM Ap_4A with $MgCl_2$. Other component present was 50 mM Tris-HCl, pH 7.5. $T = 23$ °C.

Table 2: Stoichiometries, Dissociation Constants, and Enhancement Factors of Metal−Nucleotide and Metal−Enzyme Complexes[a]

	Ap_4A			Ap_4A pyrophosphatase		
metal cation	n	K_d(mM)	ϵ_b	n	K_d(mM)	ϵ_b
Mn^{2+}	1.0	0.430 ± 0.160	2.6 ± 0.8	1.92 ± 0.32	1.1 ± 0.3	12.9−3.2
Mg^{2+}	1.0	3.9 ± 0.5[b]		2.0	8.6 ± 2.1[b]	
Ca^{2+}	1.0	2.1 ± 0.2[b]		2.0	4.3 ± 1.3[b]	

[a] Determined by PRR and EPR at 23 °C. [b] Determined by PRR in competition with Mn^{2+}.

(Figure 1A). The average value of 430 ± 160 μM was used to determine the concentrations of free Mn^{2+} in the kinetic experiments. In addition, the PRR data yielded an enhancement factor ϵ_b of 2.6 ± 0.8 for the binary Mn^{2+}·Ap_4A complex (Table 2). For small Mn^{2+} complexes, the ϵ_b values scale with the molecular weight (*20*). Since the ratio of molecular weights of $(H_2O)_3Mn^{2+}$·Ap_4A and $(H_2O)_3Mn^{2+}$·ATP is 1.59, the ϵ_b is reasonable because it is 1.53 times the ϵ_b value of the $(H_2O)_3Mn^{2+}$·ATP complex (1.7 ± 0.1) (*30*).

The dissociation constant of the Mg^{2+}·Ap_4A complex was determined by competition with Mn^{2+}. Titrations of a mixture of 0.40 mM $MnCl_2$ and 0.70 mM Ap_4A with 0−132 mM $MgCl_2$ showed a decrease in the observed enhancement factor

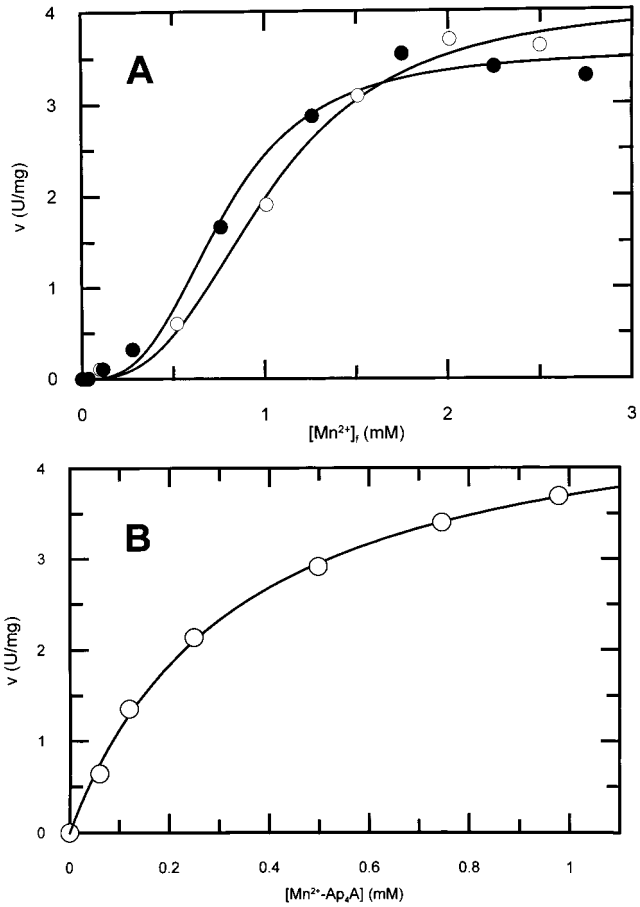

FIGURE 2: Mn^{2+} activation of Ap_4A pyrophosphatase. (A) Specific activity as a function of free Mn^{2+} concentration at total Ap_4A concentrations of 0.75 mM (●) and 1.0 mM (○). (B) Specific activity as a function of Mn^{2+}·Ap_4A concentration at a total Mn^{2+} concentration of 3 mM. Other components present were 50 mM Tris-HCl, pH 7.5, and 9 units of calf intestinal alkaline phosphatase. $T = 23$ °C.

ϵ* to a value approaching 1.0 as Mn^{2+} was displaced from the Mn^{2+}·Ap_4A complex by Mg^{2+} (Figure 1B), a result verified by EPR, which showed an increase in free Mn^{2+} concentration. From an analysis of this titration, the dissociation constant of the Mg^{2+}·Ap_4A complex was found to be 3.9 ± 0.5 mM (Table 2).

Similar titrations of the Mn^{2+}·Ap_4A mixture with 0−90.3 mM $CaCl_2$ monitored by PRR and EPR showed the complete displacement of Mn^{2+} by Ca^{2+} and yielded a dissociation constant of 2.1 ± 0.2 mM for the Ca^{2+}·Ap_4A complex (Table 2).

Mn^{2+} Activation of Ap_4A Pyrophosphatase. The rate of a metal-activated enzyme-catalyzed reaction at constant substrate concentration is typically a hyperbolic function of the free metal ion concentration (*31*). However, Figure 2A shows that Ap_4A pyrophosphatase activity as a function of free Mn^{2+} concentration is sigmoidal. The free Mn^{2+} concentration was calculated by using the K_d for the Mn^{2+}·Ap_4A complex of 430 μM, which was determined by EPR and PRR. The sigmoidal activation curve precluded the determination of Michaelis constants for free Mn^{2+}. However, a fit of the data to the Hill equation yielded an average Hill coefficient of 3.0 ± 0.2, a $K_{0.5}$ of 0.93 ± 0.35 mM, and a maximum velocity of 5.0 ± 0.8 units/mg or a k_{cat} of 1.7 ± 0.3 s^{-1} (Table 3). The Hill coefficient of 3.0 for free Mn^{2+}

Table 3: Kinetic Constants of Metal Activation of Ap_4A Pyrophosphatase[a]

metal cation	n_H	$K_{0.5}^{M2+}$ (mM)	$K_m(M^{2+}\cdot Ap_4A)$ (mM)	k_{cat} (s^{-1})	K_i [b] (mM)
Mn^{2+}	3.0 ± 0.2	0.93 ± 0.35	0.340 ± 0.025	1.7 ± 0.3	
Mg^{2+}	1.6 ± 0.3	5.3 ± 0.9	0.345 ± 0.026	0.84 ± 0.09	
Ca^{2+}					1.9 ± 1.3

[a] $T = 23$ °C. [b] Determined by competition with Mn^{2+}.

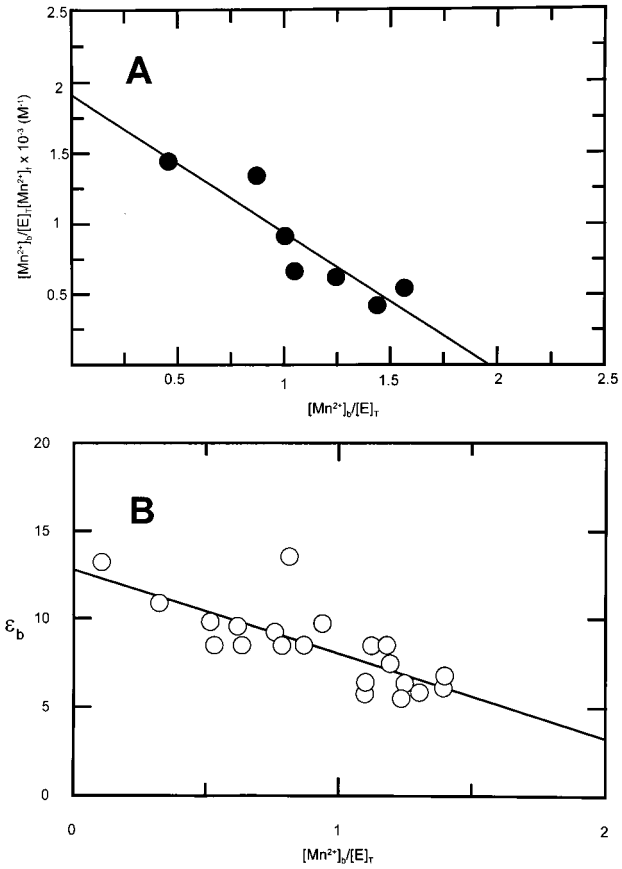

FIGURE 3: Mn^{2+} binding to Ap_4A pyrophosphatase. (A) Scatchard plot of Mn^{2+} binding to 0.4 mM enzyme. (B) Enhancement due to bound Mn^{2+} (ϵ_b) as a function of Mn^{2+} site occupancy. Other components and conditions are as in Figure 1.

indicates that at least three Mn^{2+} binding sites must be occupied to activate the enzyme. Under conditions of high Mn^{2+} concentration (3.0 mM) and varying Ap_4A up to 1 mM, a hyperbolic curve was obtained, yielding an apparent K_m for the substrate of 340 ± 25 μM expressed in terms of total Ap_4A (data not shown). At concentrations of free Ap_4A exceeding 200 μM, inhibition was seen, suggesting that *free* Ap_4A is an inhibitor and $Mn^{2+}\cdot Ap_4A$ is the true substrate. Redetermination of the K_m in terms of $Mn^{2+}\cdot Ap_4A$ yielded a value of 340 μM, in agreement with that found for total Ap_4A (Figure 2B). Thus, the kinetic data indicate that activation of Ap_4A pyrophosphatase by Mn^{2+} involves at least three metal binding sites, one of which is on the Ap_4A substrate.

Binding of Mn^{2+} to Ap_4A Pyrophosphatase. A Scatchard plot of Mn^{2+} binding to the enzyme based upon EPR data (Figure 3A) yielded a stoichiometry of 1.9 ± 0.3 sites, with dissociation constants of 1.1 ± 0.3 mM. Thus, the dissociation constants of Mn^{2+} from these two binding sites agree well with the kinetically determined $K_{0.5}$ for Mn^{2+} (0.93 mM), suggesting that both of these sites are essential for catalysis. In addition, the enzyme was found to greatly enhance the paramagnetic effect of Mn^{2+} on the water proton relaxation rate. However, as the site occupancy by Mn^{2+} increased, EPR and PRR measurements showed a large decrease in ϵ_b, the enhancement factor due to enzyme-bound Mn^{2+} (Figure 3B). These changes permitted extrapolation of ϵ_b to zero Mn^{2+} occupancy where $\epsilon_b = 12.9$, which represents the enhancement factor of the first Mn^{2+} to be bound. Extrapolation of ϵ_b to a bound Mn^{2+} occupancy of 2.0 yielded $\epsilon_b = 3.2$, which represents the average ϵ_b value of both enzyme-bound Mn^{2+} ions (Figure 3B). Because negative ϵ_b values are physically impossible (*20*), the average ϵ_b of 3.2 for both bound Mn^{2+} ions requires the ϵ_b value of the first Mn^{2+} bound to decrease as the second Mn^{2+} binding site becomes occupied. Hence, these data require site−site interaction between the two enzyme-bound Mn^{2+} ions, which decreases their paramagnetic effects on water protons. While such decreases in proton relaxation rates could have resulted from a decrease in the number of fast-exchanging water ligands on the first Mn^{2+} when the second Mn^{2+} binds, they result most simply from a decrease in the correlation time for the Mn^{2+}−water dipolar interaction. This dipolar correlation time is dominated by the longitudinal electron spin relaxation time (τ_s) of bound Mn^{2+}, which decreases due to cross-relaxation with the nearby second bound Mn^{2+} (*32*). Such cross-relaxation effects are inversely related to the sixth power of the distance between the two bound Mn^{2+} ions. Assuming such a mechanism, we may use the cross-relaxation equation (eq 7) to estimate the distance between the two bound Mn^{2+} ions (*32*):

$$\Delta\left(\frac{1}{\tau_S}\right) = \frac{2}{15}\left[\frac{S(S+1)\gamma_{Mn^{2+}}^4 h^2}{4\pi^2 r^6}\right]\tau_S^* \qquad (7)$$

In eq 7, S is the electron spin quantum number of Mn^{2+}, g is the gyromagnetic ratio of Mn^{2+}, h is Planck's constant, which are known physical constants (*21*), $\Delta(1/\tau_S)$ is the increase in the electron spin relaxation rate of bound Mn^{2+} at site 1 when a second Mn^{2+} has bound, τ_S^* is the shortened electron spin relaxation time of Mn^{2+} in the $E(Mn^{2+})_2$ complex, and r is the distance between the two bound Mn^{2+} ions. The values of $\Delta(1/\tau_S)$ and τ_S^* were calculated from the ϵ_b values and from known physical constants, using the Solomon−Bloembergen equation for longitudinal relaxation of water protons (*21*) as 1.60×10^9 s^{-1} and 5.31×10^{-10} s, respectively. Using these values in eq 7 yielded a distance of 5.9 ± 0.4 Å between the two Mn^{2+} ions, indicating their close proximity.

Mg^{2+} Activation of Ap_4A Pyrophosphatase. At concentrations of $Ap_4A \geq 1.0$ mM, activation by Mg^{2+} is sigmoidal (Figure 4). A plot of activity versus free Mg^{2+} calculated with the $Mg^{2+}\cdot Ap_4A$ dissociation constant of 3.9 mM yielded an average Hill coefficient of 1.6 ± 0.3, an average $K_{0.5}$ of 5.3 ± 0.9 mM, and a V_{max} value of 2.4 ± 0.3 units/mg or $k_{cat} = 0.84 \pm 0.09$ s^{-1} (Table 3). The Hill coefficient sets a lower limit of ≥ 2 on the number of interacting Mg^{2+} binding sites that must be occupied for catalysis. At high Mg^{2+} concentration (20 mM), enzyme activity as a function of total Ap_4A concentration was hyperbolic, yielding a K_m in terms of total Ap_4A of 410 ± 26 μM and in terms of $Mg^{2+}\cdot Ap_4A$

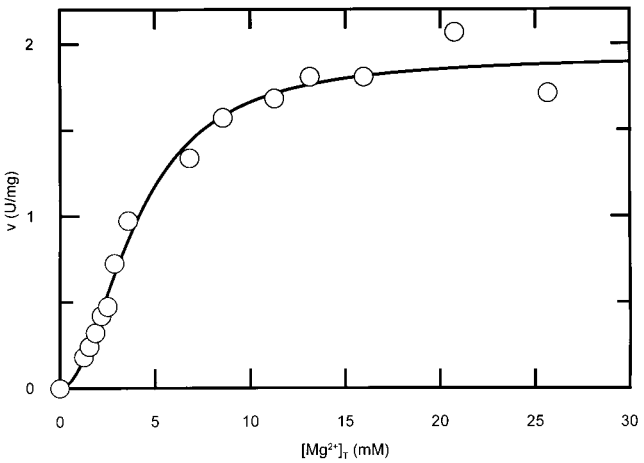

FIGURE 4: Mg^{2+} activation of Ap_4A pyrophosphatase. Specific activity is shown as a function of free Mg^{2+} concentration at a total Ap_4A concentration of 5.0 mM. The data are fitted with a Hill coefficient of 2.05 ± 0.22 and a $K_{0.5}$ of 3.91 ± 0.85 mM. At Ap_4A concentrations of 1.0, 2.0, and 7.0 mM, the Hill coefficients were 1.33 ± 0.07, 1.42 ± 0.10, and 1.58 ± 0.15, respectively, and the $K_{0.5}$ values were 6.15 ± 0.44 mM, 5.99 ± 0.66 mM, and 5.14 ± 0.73 mM, respectively. The average Hill coefficient is 1.6 ± 0.3 and the average $K_{0.5}$ is 5.3 ± 0.9 mM. Other components and conditions are as in Figure 2.

of 345 ± 26 μM. The latter value agrees with the K_m of Mn^{2+}·Ap_4A (340 ± 25 μM, Table 3) despite the order of magnitude greater affinity of Mn^{2+} for ligands in general (Table 2), suggesting that the Ap_4A-bound divalent cation does not receive ligands from the enzyme.

Mg^{2+} Binding to Ap_4A Pyrophosphatase. Since the homologous MutT pyrophosphohydrolase was found to have only one bound Mn^{2+} at the active site, our finding that Ap_4A pyrophosphatase has two Mn^{2+} binding sites was unexpected. To examine this point further, Mg^{2+} binding to Ap_4A pyrophosphatase was studied by competition with Mn^{2+}. Titration with $MgCl_2$ of solutions containing enzyme (0.4−0.8 mM) and $MnCl_2$ (0.4−0.5 mM) progressively decreased the site occupancy by Mn^{2+}, as indicated by a decrease in the observed enhancement factor ϵ* to a value approaching 1.0 (Figure 5A) and by an increase in free Mn^{2+}, independently measured by EPR. Thus, Mg^{2+} completely displaced Mn^{2+} from both of its binding sites on the enzyme. Analysis of such titrations yielded a dissociation constant for Mg^{2+} from both sites of 8.6 ± 2.1 mM (Table 2). This value is comparable to the $K_{0.5}$ value of 5.3 ± 0.9 mM obtained by kinetic analysis of the Mg^{2+}-activated enzyme (Table 3).

Inhibition of Ap_4A Pyrophosphatase by Ca^{2+}. Although not an activator (Table 1), Ca^{2+} was found to be an inhibitor of Ap_4A hydrolysis. Control experiments showed that Ca^{2+} did not inhibit the coupling enzyme, alkaline phosphatase. In a kinetic experiment with a constant Ap_4A concentration of 1 mM, in which the Ca^{2+} concentration was varied from 0 to 50.0 mM at each of three Mn^{2+} concentrations of 3.0, 6.0, and 9.0 mM, the concentration of Ca^{2+} required for half-maximal inhibition was found to increase with increasing Mn^{2+} (data not shown). This finding and the observation that complete inhibition occurs at high Ca^{2+} suggest competitive binding of Ca^{2+} and Mn^{2+}. Assuming simple competition between Ca^{2+} and Mn^{2+} yielded a K_i = 1.9 ± 1.3 mM. The unusual variability in the K_i likely resulted from the complexity of the sigmoidal activation kinetics by Mn^{2+}.

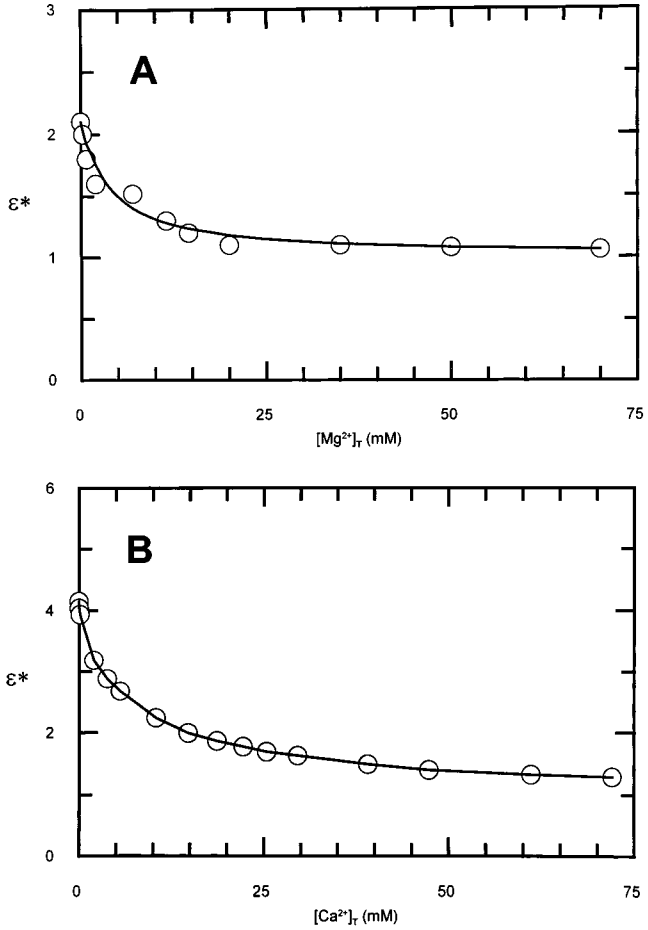

FIGURE 5: Displacement of Mn^{2+} from Ap_4A pyrophosphatase by (A) Mg^{2+} or (B) Ca^{2+} monitored by the enhancement (ϵ*) of the PRR. Components present in panel A were 0.8 mM enzyme and 0.4 mM $MnCl_2$ and in panel B were 0.4 mM enzyme and 0.5 mM $MnCl_2$. Other components and conditions were as in Figure 1. Titrations were carried out with constant concentrations of all components except $MgCl_2$ or $CaCl_2$.

Simple competition between Mn^{2+} and Ca^{2+} was demonstrated independently by direct binding studies (see next section).

Competition between Ca^{2+} and Mn^{2+} Binding to Ap_4A Pyrophosphatase. Figure 5B shows a titration of enzyme (0.4 mM) and $MnCl_2$ (0.5 mM) with $CaCl_2$ in which Ca^{2+} completely displaces Mn^{2+} from its complex with Ap_4A pyrophosphatase as indicated by the decrease in ϵ* to unity. This finding was confirmed by an increase in free Mn^{2+} detected by EPR. From this titration, the K_d of Ca^{2+} from the enzyme was calculated to be 4.3 ± 1.3 mM. As noted above, the dissociation constant of the binary Ca^{2+}·Ap_4A complex was found by similar methods to be 2.1 ± 0.2 mM (Table 2). These values are comparable to the K_i value of 1.9 ± 1.3 mM detected kinetically, suggesting that inhibition by Ca^{2+} results from the complete displacement of Mn^{2+} from the active site. The failure of Ca^{2+} to activate Mg^{2+}-activated enzymes, despite its ability to bind to the same sites, was first demonstrated with pyruvate kinase (*30*) and is quite common. It may be ascribed most simply to the larger ionic radius of Ca^{2+} (1.18 Å) compared to Mg^{2+} (0.82 Å), Mn^{2+} (0.80 Å), and Zn^{2+} (0.88 Å) (*33*), which precludes its optimum positioning for catalysis. Conversely, staphylococcal nuclease is activated solely by Ca^{2+}. Mn^{2+} and Co^{2+}

Ap_4A pyrophosphatase	52	**G**GIDEG**E**EPLDAAR**REL**Y**EE**T**G**M	74
MutT pyrophosphohydrolase	38	**G**KIEMG**E**TPEQAVV**REL**Q**EE**V**G**I	60

FIGURE 6: Comparison of the Nudix box sequence of the Ap_4A pyrophosphatase (*7*) with that of the MutT pyrophosphohydrolase (*1*). Conserved residues are shown in boldface type. Underlined residues are potential metal ligands in Ap_4A pyrophosphatase that are not found in the MutT enzyme.

compete with Ca^{2+} but fail to activate, presumably because they are too small (*34*, *35*).

DISCUSSION

The most interesting and surprising result of these studies is that, unlike the MutT enzyme, which requires two divalent cations for activity,[2] Ap_4A pyrophosphatase, which also has a Nudix box, requires a total of three divalent cations for activity—two bound to the enzyme and one bound to the Ap_4A substrate. This stoichiometry was demonstrated kinetically by a Hill coefficient of 3 in the activation of the enzyme by free Mn^{2+} and by direct binding studies, which revealed two Mn^{2+} binding sites on the enzyme and one on the substrate with dissociation constants in reasonable agreement with the kinetically determined $K_{0.5}$ for Mn^{2+}. The unexpected stoichiometry was confirmed by competitive metal binding studies with the activator Mg^{2+} and the inhibitor Ca^{2+}, each of which competed with Mn^{2+} at both of its sites on the enzyme and at its site on the substrate. Activation by Mg^{2+} is less cooperative than activation by Mn^{2+}, as reflected in the lower Hill coefficient of 1.6 for Mg^{2+} (Table 1). This difference in cooperativity may result from the order of magnitude lower affinities of Mg^{2+} for both Ap_4A and Ap_4A pyrophosphatase (Table 2).

Cooperative activation by divalent cations has previously been found with the 3′,5′-exonuclease of DNA polymerase I (*36*) due to the formation of a binuclear $E(M^{2+})_2$ complex in which the two metal ions share a common Asp ligand (*37*). The two enzyme-bound Mn^{2+} ions in Ap_4A pyrophosphatase are near enough to each other (5.9 ± 0.4 Å) to interact magnetically but probably not near enough to share a common liganding residue, which typically requires a proximity of 4.0 Å as on alkaline phosphatase (*38*). Hence, additional metal−liganding residues should be present on Ap_4A pyrophosphatase that are absent on the MutT pyrophosphohydrolase, since the latter, which is also a Nudix enzyme, requires a total of only two divalent cations for activity, one on the enzyme and one on the NTP substrate (*2*, *17*).[2]

On MutT, the enzyme-bound metal ion binds near the Nudix box and is coordinated by three conserved residues within the Nudix box, Gly-38 and the carboxylate side chains of Glu-56 and Glu-57, as well as by a nonconserved residue outside the Nudix box on loop III, Gly-98 (*2*). Because of the proximity of the two metal binding sites on Ap_4A pyrophosphatase, we looked for additional possible metal

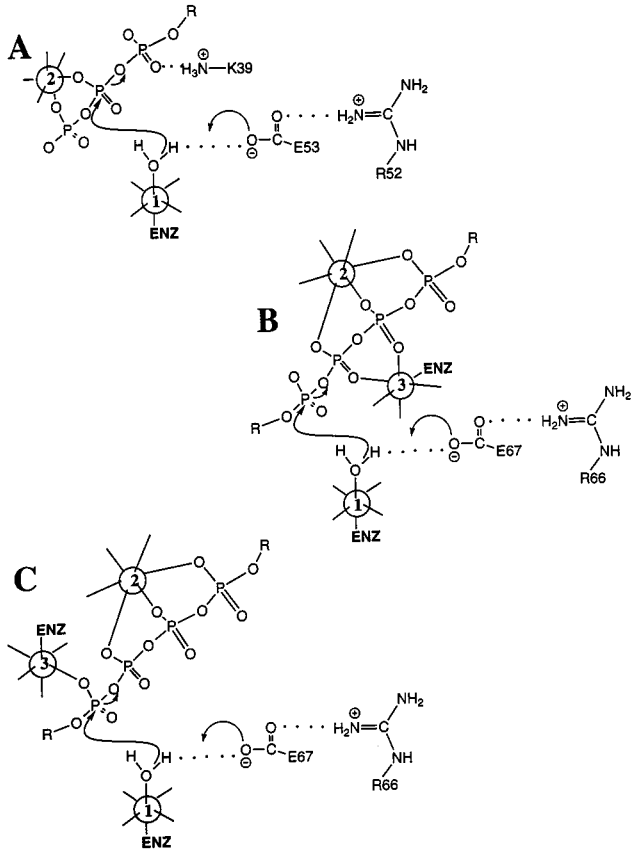

FIGURE 7: Mechanisms of Nudix enzymes. (A) Mechanism of the MutT pyrophosphohydrolase showing the role of the enzyme-bound divalent cation (**1**) and the nucleotide-bound divalent cation (**2**) (*2*, *3*, *39*). (B) Proposed mechanism of Ap_4A pyrophosphatase showing the roles of the two enzyme-bound divalent cations (**1** and **3**) and the nucleotide-bound divalent cation (**2**). (C) Alternative mechanism of Ap_4A pyrophosphatase showing a different role of the enzyme-bound metal (**3**).

ligands in the Nudix box sequence of Ap_4A pyrophosphatase that are not conserved in the sequence of the MutT enzyme. Candidate residues were two glutamates and one aspartate in Ap_4A pyrophosphatase, which correspond to Met-42, Thr-45, and Gln-48 of MutT (Figure 6). Model building of these potential liganding residues into the MutT structure showed that Glu residues at position 42 and possibly at position 45 of loop I could coordinate a second metal ion at a distance of 5.9 ± 0.4 Å from the bound metal ion. However, an Asp at position 48 (in helix I) is too far away by ~10 Å to do so. Structural and mutagenesis studies of Ap_4A pyrophosphatase will be required to establish the roles, if any, of these nonconserved acidic residues.

The catalytic role of the single enzyme-bound divalent cation in the MutT pyrophosphohydrolase (Figure 7A, metal **1**) is to present a water or hydroxyl nucleophile to attack the β-phosphorus of the M^{2+}•NTP substrate, displacing the NMP leaving group (*2*, *3*) (Figure 7A). Subsequently, the metal coordinates the pyrophosphate product (*3*, *39*). On Ap_4A pyrophosphatase, we suggest that one of the two

[2] We have reexamined by EPR and PRR measurements and confirmed ref *17* that the MutT enzyme binds only one Mn^{2+} ion tightly with a dissociation constant comparable to its kinetically determined activator constant (G. Wu and A. S. Mildvan, unpublished observations, 1999). We also found no evidence for tightly bound Zn^{2+} in the MutT enzyme by atomic absorption spectroscopy (J. Lin and A. S. Mildvan, unpublished observations, 1996) or for tightly bound paramagnetic metal ions by PRR studies of the MutT enzyme (G. Wu and A. S. Mildvan, unpublished observations, 1999).

enzyme-bound metal ions plays the same role, to present a water or hydroxyl nucleophile to attack the δ-phosphorus of Ap_4A, displacing ATP as the leaving group, and subsequently to coordinate the AMP product (Figure 7B, metal **1**). The second enzyme-bound metal on Ap_4A pyrophosphatase, which is absent in MutT pyrophosphohydrolase (Figure 7B, metal **3**), together with the Ap_4A-bound metal (**2**) may facilitate the departure of the highly negatively charged ATP leaving group by charge neutralization. In this connection, it is of interest that the positively charged Lys-39, which facilitates the departure of the NMP leaving group in the MutT reaction (Figure 7A) (*2*), contributing a factor of ∼40 to the k_{cat}/K_m (*40*), is replaced by a neutral Gly in Ap_4A pyrophosphatase; yet the catalytic powers of the two enzymes (∼10^9) are very similar. Alternatively, as shown in Figure 7C, the second enzyme-bound divalent cation on Ap_4A pyrophosphatase may coordinate the δ-phosphoryl group of Ap_4A, facilitating attack at this position by increasing its electrophilicity, and subsequently coordinate the AMP product. Detailed structural and kinetic studies with appropriate mutants will be needed to clarify the precise role of the additional metal, which may be allosteric. Regardless of the role, it is now clear that different Nudix enzymes require different numbers of divalent cation activators, depending on the precise nature of the substrate and the reaction that is catalyzed.

REFERENCES

1. Bessman, M. J., Frick, D. N., and O'Handley, S. F. (1996) *J. Biol. Chem. 271*, 25059−25062.
2. Lin, J., Abeygunawardana, C., Frick, D. N., Bessman, M. J., and Mildvan, A. S. (1997) *Biochemistry 36*, 1199−1211.
3. Mildvan, A. S., Weber, D. J., and Abeygunawardana, C. (1999) *Adv. Enzymol. Relat. Areas Mol. Biol. 73*, 183−207.
4. Ihler, G. M. (1996) *FEMS Microbiol. Lett. 144*, 1−11.
5. Mitchell, S. J., and Minnick, M. F. (1995) *Infect. Immun. 63*, 1552−1562.
6. Krueger, C. M., Marks, K. L., and Ihler, G. M. (1995) *J. Bacteriol. 177*, 7271−7274.
7. Conyers, G. B., and Bessman, M. J. (1999) *J. Biol. Chem. 274*, 1203−1206.
8. Cartwright, J. L., Britton, P., Minnick, M. F., and McLennan, A. G. (1999) *Biochem. Biophys. Res. Commun. 256*, 474−479.
9. Maksel, D., Guranowski, A., Ilgoutz, S. C., Moir, A., Blackburn, M. G., and Gayler, K. R. (1998) *Biochem. J. 329*, 313−319.
10. Huang, Y., Garrison, P. N., and Barnes, L. D. (1995) *Biochem. J. 312*, 925−932.
11. Hankin, S., Wintero, A. K., and McLennan, A. G. (1996) *Biochem. Soc. Trans. 24*, 418S.
12. Feussner, K., Guranowski, A., Kostka, S., and Wasternack, C. (1996) *Z. Naturforsch. C 51*, 477−486.
13. Garrison, P. N., Roberson, G. M., Culver, C. A., and Barnes, L. D. (1982) *Biochemistry 21*, 6129−6133.
14. Hohn, M., Albert, W., and Grummt, F. (1982) *J. Biol. Chem. 257*, 3003−3006.
15. Guranowski, A., Starzynska, E., Taylor, G. E., and Blackburn, G. M. (1989) *Biochem. J. 262*, 241−244.
16. Kisselev, L. L., Justesen, J., Wolfson, A. D., and Frolova, L. Y. (1998) *FEBS Lett. 427*, 157−163.
17. Frick, D. N., Weber, D. J., Gillespie, J. R., Bessman, M. J., and Mildvan, A. S. (1994) *J. Biol. Chem. 269*, 1794−1803.
18. Bhatnagar, S. K., Bullions, L. C., and Bessman, M. J. (1991) *J. Biol. Chem. 266*, 9050−9054.
19. Lin, J., Abeygunawardana, C., Frick, D. N., Bessman, M. J., and Mildvan, A. S. (1996) *Biochemistry 35*, 6715−6726.
20. Mildvan, A. S., and Cohn, M. (1970) *Adv. Enzymol. Relat. Areas Mol. Biol. 33*, 1−70.
21. Mildvan, A. S., and Engle, J. L. (1972) *Methods Enzymol. 26*, 654−682.
22. Ames, B. N., and Dubin, D. T. (1960) *J. Biol. Chem. 235*, 769−775.
23. Cohn, M., and Townsend, J. (1954) *Nature 173*, 1090−1091.
24. Carr, H. Y., and Purcell, E. M. (1954) *Phys. Rev. 94*, 630−638.
25. Lansdown, A. B. G., Sampson, B. and Rowe, A. (1999) *J. Anat. 195*, 375−386.
26. Connell, P., Young, V. M., Toborek, M., Cohen, D. A., Barve, S., McClain, C. J., and Hennig, B. (1997) *J. Am. Coll. Nutr. 16*, 411−417.
27. Hoch, F. L. and Vallee, B. L. (1952) *J. Biol. Chem. 195*, 531−540.
28. Ash, D. E. and Schramm, V. L. (1982) *J. Biol. Chem. 257*, 9261−9264.
29. Mildvan, A. S. (1987) *Magnesium 6*, 28−33.
30. Mildvan, A. S., and Cohn, M. (1966) *J. Biol. Chem. 241*, 1178−1193.
31. Dixon, M., and Webb, E. C. (1979) *Enzymes (3rd Ed.)*, Academic Press, New York.
32. Gupta, R. K. (1977) *J. Biol. Chem. 252*, 5967−5976.
33. Weast, R. C. (1988) *CRC handbook of chemistry and physics*, 1st student ed., CRC Press, Boca Raton, FL.
34. Serpersu, E. H., Shortle, D., and Mildvan, A. S. (1986) *Biochemistry 25*, 68−77.
35. Serpersu, E. H., McCracken, J., Peisach, J., and Mildvan, A. S. (1988) *Biochemistry 27*, 8034−8044.
36. Han, H., Rifkind, J. M., and Mildvan, A. S. (1976) *Biochemistry 30*, 11104−11108.
37. Freemont, P. S., Friedman, J. M., Beese, L. S., Sanderson, M. R., and Steitz, T. A. (1988) *Proc. Natl. Acad. Sci. U.S.A. 85*, 8924−8928.
38. Steitz, T. A., and Steitz, J. A. (1993) *Proc. Natl. Acad. Sci. U.S.A 90*, 6498−6502.
39. Harris, T. K., Wu, G., Massiah, M. A., and Mildvan, A. S. (2000) *Biochemistry* (in press).
40. Frick, D. N., Weber, D. J., Abeygunawardana, C., Gittis, A. G., Bessman, M. J., and Mildvan, A. S. (1995) *Biochemistry 34*, 5577−5586.

BI992458N